

TECHNIQUES OF RAY AVERAGING

HOWARD N. SOUTHGATE

Hydraulics Research Station Limited, Wallingford, Oxon, OX10 8BA, U.K.

SUMMARY

Ray methods are used in coastal and harbour wave disturbance investigations where the area to be modelled is large compared to the wavelength. The interpretation of forward-plotted ray diagrams, once obtained, has always been a difficult problem. The technique described in this paper calculates wave amplitudes during the ray plotting process and requires only minor modifications to existing ray plotting programs. The idea is to superimpose a grid of square elements over the entire sea area under study, and to perform a spatial averaging of the rays crossing each square element. This 'square-averaging' technique has a number of advantages. It smooths the rapid amplitude variations near caustics, calculates the interference of several wave trains, and generates amplitudes automatically in a square array covering the whole studied sea area. Two types of sensitivity tests are carried out. These tests are designed to determine the accuracy of the predicted wave amplitudes with respect to: (1) the square size per wavelength, and (2) the ray density. These two factors largely determine the computing storage, time and cost of a ray model. An upper limit on the square size per wavelength and a lower limit on the ray density are obtained.

KEY WORDS Ray Methods Water Waves Refraction Diffraction Coasts Harbours

1. INTRODUCTION

Ray methods have traditionally been used by coastal engineers to determine the effects of refraction and shoaling of sea waves as they approach the shoreline. More recently, the theory underlying ray methods has been extended to include diffraction of sea waves by some simple breakwater arrangements commonly found at harbour entrances. Reflections from harbour boundaries can also be modelled by ray methods. These developments have enabled ray methods to be used for studying the wave disturbance in outer harbour areas.^{1,2}

Ray methods are restricted to modelling linear wave phenomena, and do not incorporate 'internal' diffraction processes (i.e. diffraction other than by surface obstacles). It may seem at first sight therefore that alternative solution techniques which can incorporate more of the physical processes affecting waves are preferable. Harbour models based on finite-difference^{3,4} or finite-element⁵⁻⁷ techniques are able to incorporate the combined primary wave effects of refraction, diffraction and reflections and, depending on the governing equations, some non-linear effects as well. However, a minimum number of grid points per wavelength (generally about six) are required in order to resolve the waves. For short waves in large harbour areas this restriction can result in excessively high data preparation time, computing storage and run time. Ray methods, on the other hand, can use far larger element sizes per wavelength. For coastal problems, parabolic methods^{8,9} which can include diffraction effects (but not the effects of reflected waves) are appropriate. These methods use a 'marching' solution technique which is considerably quicker than those techniques which require simultaneous solution. However, there is again a lower limit to the number of grid

points per wavelength, and for very large areas (of the order of hundreds of wavelengths) ray methods are still essential. Ray methods, therefore, are indispensable for practical harbour and coastal wave disturbance problems where the size of the area to be modelled is large compared to the wavelength.

In this paper 'forward' ray methods only are considered, i.e. those which involve plotting rays shorewards in the direction of wave propagation. In coastal problems, an alternative technique of reverse projection of rays from an inshore point out to deep water is often used.¹⁰ In this technique, an offshore wave spectrum in period and direction is specified, and the inshore spectrum is calculated from the condition that spectral density is conserved along each ray. This technique has the advantage of eliminating anomalies such as caustics which appear in 'forward' ray diagrams. This is because caustics will make only a small contribution to the statistical quantities (such as significant wave height and zero-crossing period) determined from a wave spectrum. Diffraction and dissipation effects are not modelled in this method.

The computational process of a 'forward' ray method involves plotting sets of closely spaced rays over the sea area of interest, with each set of rays representing one wave train. The sea area is discretized into a grid of rectangular or triangular elements, and depth data is taken at the grid intersections. In the refraction program used by the author,¹¹ the assumption is made that the wave celerity varies linearly within each grid element. This approximation is quite adequate for practical applications and allows a quick means of plotting rays over the sea area.

In principle, the determination of the wave field at any point is simple. The wave amplitude of one wave train is calculated from the condition of conservation of energy flux between neighbouring rays, and the wave phase is obtained by integration of the wave number along a ray. At points where there are two or more intersecting wave trains, the total wave field is calculated from the linear superposition of the component waves. In practice, however, a typical ray diagram shows a mess of rays with many crossings and caustics, and the interpretation of these diagrams presents a difficult problem. It is possible to calculate refraction and shoaling coefficients along individual rays without reference to the behaviour of neighbouring rays.^{10,12} This method, however, will break down near important areas of 'internal' diffraction and will not calculate the interference between two or more wave trains.

As a general rule, it is preferable to use some kind of spatial averaging of rays to attempt to take account of the trends of bundles of rays rather than the behaviour of individual rays. This consideration applies in particular to the spatial averaging method described in this paper. In this method, a grid composed of square elements is superimposed over the sea area under study, and the effects of rays passing through each square element are averaged. The averaged wave heights and phases thus found are assumed to be the values at the centres of the square elements. The results obtained are therefore in the form of a square array of spot wave heights and phases covering the whole studied sea area. The computational process will be greatly simplified if the grid used in this spatial averaging process is chosen to coincide with the grid holding the depth information and in which ray paths are plotted. In what follows it will be assumed that the two grids are identical, but it should be remembered that they are distinct conceptually. This 'square-averaging' technique turns out to have a number of favourable features which are listed below.

1. Near caustics and ray crossings, the square-averaging technique has the effect of smoothing the rapid variation of wave height obtained from single-ray methods.
2. The square-averaging method calculates the resultant of two or more intersecting wave trains with the options of either taking into account the relative phases or of treating them as random.

3. When phasing is taken into account, wave heights will be predicted correctly if squares are only partially covered by a set of rays. As shown later, this fact is important when modelling waves diffracted by a single breakwater.
4. Results are automatically generated in a regular array over the whole sea area of interest. This is of particular importance in harbour modelling where it is often required to find the most sheltered positions for ship berths, etc.

It is possible to perform a spatial averaging of rays over a line instead of a square. The theories of the two methods are very similar, but the line-averaging method has the disadvantage of breaking down when rays make a very acute angle with the line. Some spatial averaging methods using line-averaging have already been put forward.^{13,14} These methods, however, only consider the case where the relative phases of intersecting wave trains are random.

The purpose of this paper is to develop the theory of square-averaging and to analyse the sensitivity of results to the chosen square size per wavelength and ray density. The computing time (and cost) of any ray model is dependent on both these factors. The sensitivity analysis aims to determine the trends in wave amplitude error with respect to each of these factors. Upper limits on the square size per wavelength and lower limits on the ray density are obtained.

2. THE RAY APPROXIMATION

The surface water waves are assumed to be time-harmonic and to have small amplitudes, so that linear water-wave theory applies. The propagation of these waves over a gently sloping sea bed is described by solutions to the reduced equation

$$\nabla \cdot (cc_g \nabla \eta) + \frac{\omega^2 c_g}{c} \eta = 0 \quad (1)$$

with the appropriate boundary conditions.^{15,16} In this equation c is the wave celerity, c_g the group velocity, ω the angular wave frequency, η the complex wave amplitude and ∇ the two-dimensional horizontal gradient operator. At any location, c is given implicitly by the dispersion relation

$$c = \left(\frac{g}{k} \tanh kh \right)^{1/2} \quad (2)$$

where k is the wave number ($=\omega/c$), g the acceleration due to gravity and h the water depth. The group velocity c_g is given by

$$c_g = \frac{c}{2} \left(1 + \frac{2kh}{\sinh 2kh} \right) \quad (3)$$

The complex wave amplitude η can be written as

$$\eta = Ae^{iS} \quad (4)$$

where A is the wave amplitude and S the wave phase. Substitution of equation (4) into equation (1) leads to the equations

$$(\nabla S)^2 = k^2 \quad (5)$$

$$\nabla \cdot (cc_g A^2 \nabla S) = 0 \quad (6)$$

Equation (6) is exact, but in deriving equation (5) the following conditions have been assumed to hold:

$$\frac{\nabla^2 A}{k^2 A} \ll 1 \quad (7)$$

$$\left| \frac{\nabla A}{kA} \right| \cdot \left| \frac{\nabla h}{kh} \right| \ll 1 \quad (8)$$

A derivation and discussion of conditions (7) and (8) are given in reference 17 (see also reference 18). Equations (5) and (6) are known as the ray (or refraction) equations. Note that they apply separately to different wave trains. At locations where conditions (7) or (8) do not hold for a particular wave train, diffraction of that wave train occurs and the ray approximation is no longer valid.

By applying the divergence theorem of Gauss to an area between two neighbouring rays equation (6) can be transformed (after substitution of ∇S by equation (5)) into

$$A^2 c_g b = E \quad (9)$$

b is the separation of the rays and E is a constant for a particular pair of rays. Equation (9) is the condition of conservation of energy flux between rays, and it determines the wave amplitude along each ray. The phase function is calculated by integration of equation (5) along a ray:

$$S = \int_{\text{ray}} k \, ds + S_0 \quad (10)$$

s is the path length along a ray from the ray's starting point, and S_0 is the phase at the starting point. At locations where there are two or more intersecting wave trains, the total wave field is given by the linear superposition of the component waves:

$$\eta_{\text{total}} = \sum_{\substack{\text{All wave} \\ \text{trains}}} A e^{iS} \quad (11)$$

3. THEORY OF RAY AVERAGING

The ray averaging technique is based on the spatial averaging of rays passing through a square area or across a line. The term 'with phasing' will be used to denote the case where the relative phases of separate wave trains crossing an averaging square or line are taken into account. Similarly, the term 'without phasing' will be used when separate wave trains are treated as having random relative phases. In both the square- and line-averaging methods the idea of a 'region of influence' of a ray is used. If one imagines two lines drawn on either side of a ray midway between it and its neighbouring rays, the region of influence of the ray is the area between these two lines (see Figure 1).

In this section, the theory of the square-averaging method is developed. Square-averaging with phasing and without phasing are considered separately. The arguments used in the development of the line- and square-averaging methods are identical. Therefore, formulae for the line-averaging method will simply be quoted where the corresponding formulae for square-averaging have been obtained.

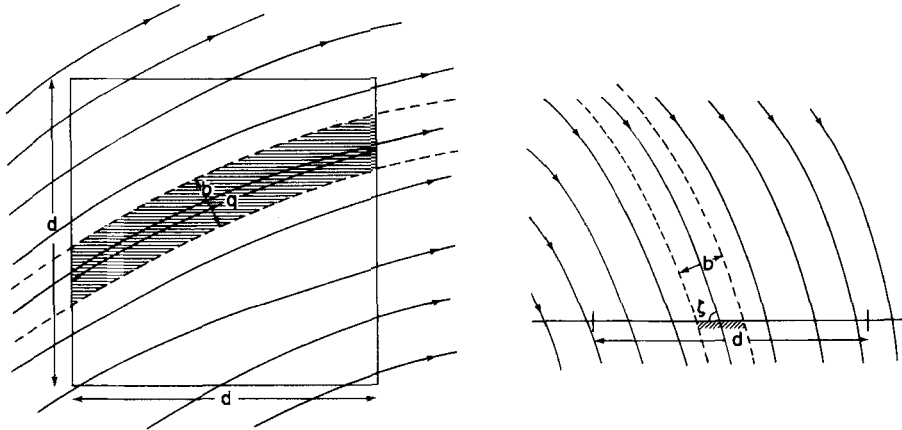


Figure 1. Square-averaging (left) and Line-averaging. The shaded area between the dashed lines is the 'region of influence' of one ray

3.1. Square-averaging with phasing

Consider several wave trains crossing an averaging square. The law of superposition (11) combined with the formula for weighted averages gives the following expression for the average wave amplitude and phase in the square.

$$A_{av}e^{iS_{av}} = \left(\frac{f_1 A_1 e^{iS_1} + f_2 A_2 e^{iS_2} + \dots}{f_1 + f_2 + \dots} \right)_1 + \left(\frac{f_1 A_1 e^{iS_1} + f_2 A_2 e^{iS_2} + \dots}{f_1 + f_2 + \dots} \right)_2 + \dots \quad (12)$$

where

A_{av} is the average wave amplitude in the square.

S_{av} is the average wave phase in the square.

Brackets denote separate wave trains.

Terms in each bracket denote rays in a particular wave train.

A_1, A_2 etc. are the average wave amplitudes of rays calculated from equation (9).

S_1, S_2 etc. are the average wave phases of rays calculated from equation (10).

f_1, f_2 etc. are the factors by which the wave amplitudes of each ray are weighted.

The basic assumption is now made that *the wave amplitude of each ray is weighted in proportion to the region of influence of the ray in the averaging square*. In other words, the f s are chosen to be

$$f = \frac{qb}{d^2} \quad (13)$$

where

q is the length of the ray in the averaging square

b is the average separation of the ray from its neighbouring rays in the averaging square

d is the length of the side of the square

qb is clearly the region of influence of the ray in the averaging square (Figure 1). Substituting equation (13) for the f s and equation (9) for the A s in equation (12):

$$A_{av}e^{iS_{av}} = \frac{1}{d^2} \left(\frac{q_1(b_1 E_1 / c_{g1})^{1/2} e^{iS_1} + q_2(b_2 E_2 / c_{g2})^{1/2} e^{iS_2} + \dots}{q_1 b_1 / d^2 + q_2 b_2 / d^2 + \dots} \right)_1 + \frac{1}{d^2} \left(\frac{q_1(b_1 E_1 / c_{g1})^{1/2} e^{iS_1} + q_2(b_2 E_2 / c_{g2})^{1/2} e^{iS_2} + \dots}{q_1 b_1 / d^2 + q_2 b_2 / d^2 + \dots} \right)_2 + \frac{1}{d^2} (\dots)_3 + \dots \quad (14)$$

For sets of rays which cover the whole averaging square the denominators in each set of brackets ($\sum qb/d^2$) are unity. Thus, each expression for the wave amplitude and phase contribution of a ray contains quantities which relate to that ray only, and not to the other rays in its wave train. The average wave amplitude and phase in an averaging square can therefore be written as

$$A_{av}e^{iS_{av}} = \frac{1}{d^2} \sum_{\substack{\text{All} \\ \text{rays}}} q \left(\frac{bE}{c_g} \right)^{1/2} e^{iS} \quad (15)$$

Precisely the same arguments are used in deriving the formula for the average wave amplitude and phase for sets of rays crossing an averaging line. The only difference is that the f s are given by (see Figure 1)

$$f = \frac{b}{d \sin \zeta} A \quad (16)$$

where

ζ is the angle between the ray and the averaging line.

d is the length of the averaging line.

This leads to the following formula for the average wave amplitude and phase:

$$A_{av}e^{iS_{av}} = \frac{1}{d} \sum_{\substack{\text{All} \\ \text{rays}}} \frac{1}{\sin \zeta} \left(\frac{bE}{c_g} \right)^{1/2} e^{iS} \quad (17)$$

It can be seen that this method will break down when rays make a very acute angle (small ζ) with the averaging line.

Each quantity on the right-hand side of equation (15) (and equation (17)) can be readily determined in a ray plotting algorithm. An average group velocity, c_g , can be found for each averaging square from equation (3). The energy flux constant, E , is specified in the initial conditions of each ray. The length of the ray, q , and the phase, S , follow from the determination of the ray path. The ray separation, b , can be found by evaluating an ordinary differential equation along each ray.^{10,12}

Average values of b and S between the ray's entry and exit points in the averaging square are used. As discussed in Section 4, this method of determining S does place an upper limit on the square size per wavelength.

It is of considerable importance computationally that the expression for the amplitude and phase contributions of a ray should be independent of other rays in its wave train. This fact means that only two result arrays (containing the real and imaginary parts of the wave field in each averaging square) are needed. If the expression for a ray's contribution *did* depend on terms involving other rays in its wave train, separate result arrays would be needed for each wave train in the problem. This could lead to a high demand on computing storage particularly in harbour problems where, in addition to the incident wave, there may be several diffracted and reflected wave trains.

Since A_{av} is inversely proportional to the area of the averaging square (d^2) in equation (15), it follows that the wave field will be predicted correctly by equation (15) when an averaging square is only partially covered by a set of rays. In other words if a set of rays covers a fraction F of an averaging square, the predicted amplitude will be F times the value obtained if the whole square had been covered. This property is essential in harbour

problems where diffraction of waves at the entrance is by a single ‘semi-infinite’ breakwater. In these types of problems, a geometric shadow boundary is present, separating the zones sheltered from and exposed to the incident wave (Figure 3). Square intersected by this boundary will be partially covered by the set of incident rays and by two sets of diffracted rays.²

3.2. Caustics and ray crossings

An interesting feature of the square- and line-averaging methods is the position of the ray separation factor, b , in equations (15) and (17). It appears in the numerator and not, as might be expected from equation (9), in the denominator. Therefore, near caustics and ray crossings as $b \rightarrow 0$ the unrealistically high wave amplitudes of single-ray methods are not obtained. The explanation is easy to see if the amplitude contribution of a ray to an averaging square is written as

$$A = \frac{qb}{d^2} \left(\frac{E}{bc_g} \right)^{1/2} \quad (18)$$

As $b \rightarrow 0$, the condition of conservation of energy flux (second term on the right) causes the amplitude to tend to infinity as $b^{-1/2}$. However, the region of influence of the ray (first term on the right) tends to zero as b . This latter effect is therefore the stronger.

This smoothing of caustics and ray crossings is similar in its effect to the actual diffraction process that always occurs around such areas, despite there being no attempt to model the mechanism of the diffraction process. Good, though not of course highly accurate, amplitude results can be expected where caustic features are contained within averaging squares. Larger scale areas of ‘internal’ diffraction cannot be expected to be modelled correctly, though even in these cases qualitative accuracy is often obtained (see, for example, References 1 and 13). Errors caused by caustics and ray crossings are often further reduced by carrying out a series of runs covering a spectrum of incident wave periods and directions.

3.3. Square averaging without phasing

For several intersecting wave trains with random relative phases the law of superposition in an averaging square is

$$A_{av}^2 = \left(\frac{f_1 A_1 + f_2 A_2 + \dots}{f_1 + f_2 + \dots} \right)_1^2 + \left(\frac{f_1 A_1 + f_2 A_2 + \dots}{f_1 + f_2 + \dots} \right)_2^2 + (\dots)_3^2 + \dots \quad (19)$$

The same basic assumption as before is made that the wave amplitude contribution of a ray is weighted in proportion to the region of influence of the ray in the averaging square. Substituting equation (13) for the f_s in equation (19):

$$A_{av}^2 = \frac{1}{d^4} \left(\frac{q_1 b_1 A_1 + q_2 b_2 A_2 + \dots}{q_1 b_1 / d^2 + q_2 b_2 / d^2 + \dots} \right)_1^2 + \frac{1}{d^4} \left(\frac{q_1 b_1 A_1 + q_2 b_2 A_2 + \dots}{q_1 b_1 / d^2 + q_2 b_2 / d^2 + \dots} \right)_2^2 + \frac{1}{d^4} (\dots)_3^2 + \dots \quad (20)$$

Because each bracket is squared, the wave amplitude contribution of each ray is dependent on terms involving other rays in its wave train. This is in contrast to equation (14) where phasing was included. As discussed in Section 3.1, it is desirable computationally that a ray’s contribution should be independent of other rays in its wave train. A formula with this computational requirement can be derived if it is assumed that the variation in amplitude between rays in each wave train in an averaging square is negligible. In other words, it is

assumed that for each wave train in an averaging square:

$$A_1 = A_2 = A_3 = \dots \quad (21)$$

The condition that rays in each wave train cover the whole of the averaging squares is also needed.

$$\sum_{\text{wave train}} \frac{qb}{d^2} = 1 \quad (22)$$

Using equations (21) and (22), equation (20) can be written as

$$A_{\text{av}}^2 = \frac{1}{d^2} (q_1 b_1 A_1^2 + q_2 b_2 A_2^2 + \dots)_1 + \frac{1}{d^2} (q_1 b_1 A_1^2 + q_2 b_2 A_2^2 + \dots)_2 + \frac{1}{d^2} (\dots)_3 + \dots \quad (23)$$

In this formula, the contribution of each ray is now independent of other rays in its wave train. Substituting equation (9) for the A s:

$$A_{\text{av}} = \frac{1}{d} \left(\sum_{\text{rays}} \frac{qE}{c_r} \right)^{1/2} \quad (24)$$

The corresponding formula for sets of rays crossing an averaging line is derived in an identical way:

$$A_{\text{av}} = \frac{1}{\sqrt{d}} \left(\sum_{\text{rays}} \frac{E}{c_g \sin \zeta} \right)^{1/2} \quad (25)$$

Since A_{av} is not inversely proportional to the area of the averaging square in equation (24) (or to the length of the averaging line in equation (25)) it follows that the wave field will *not* be predicted correctly when an averaging square is only partially covered by a set of rays. Two situations where partial covering of squares could occur are outlined below. In neither case, however, will the incorrect prediction of wave amplitude be important.

1. In problems involving diffraction by a single breakwater, the averaging squares intersected by the shadow boundary are partially covered by three sets of rays (see Figure 3). However, since these sets of rays are phase-locked, it is essential that square averaging *with* phasing should be used.
2. Irregularities or sharp boundaries in an obstacle will produce reflected waves with truncated crests in a ray method. The sets of rays at the ends of these crests will only partially cover the squares through which they pass. The errors that will be introduced by this will, however, be masked by the more important (and unavoidable) error that diffraction which is always present at truncated wave crests will not be modelled.

In most practical coastal and harbour problems it is envisaged that square averaging without phasing is used for the interference of reflected waves with direct waves. It is usually possible to obtain a reasonable estimate of the amplitude reflection coefficient of a boundary, either by model tests or the use of semi-empirical formulae. However, the phase change undergone on reflection is often unknown except for the simplest types of boundary (such as a straight vertical wall). The inclusion of the relative phases of direct and reflected waves gives an interference pattern with large spatial variations in the total wave amplitude. Obviously, the phase change undergone on reflection would need to be known with considerable accuracy for such predicted wave amplitudes to be realistic. Square-averaging without phasing, on the other hand, would tend to give a smooth spatial variation of the total wave amplitude.

4. SENSITIVITY OF SQUARE AVERAGING TO SIZE OF SQUARES

In the square-averaging formula with phasing, equation (15), the average of the phases of each ray at the entry and exit points in an averaging square is used. Figure 2 shows the simple case of one set of parallel rays with no refraction crossing an averaging square. It can be seen that the mean phase of each ray is different from the correct value at the centre of the square. The larger the square size relative to the wavelength, the greater will be the error introduced by taking the mean phase of each ray. It is therefore important to determine how the square size affects the accuracy of the predicted wave amplitudes, and to determine the maximum limit of square size per wavelength for use in practical problems. Clearly, this consideration does not apply to square-averaging without phasing.

This square size sensitivity analysis is carried out for three cases:

1. A single set of parallel rays with no refraction (Figure 2).
2. Several intersecting sets of rays (parallel and diverging) and no refraction (Figure 3).
3. As (1), but with refraction present (Figure 9).

It was thought that an improvement could be made to the calculation of the mean phase by extrapolating a ray's path on to the circumcircle of each averaging square (Figure 11). An average of the phases at the intersections of the ray with the circumcircle would be used. This idea proved to be very successful and to increase considerably the maximum limit on the square size per wavelength. The method, and the results obtained from it, are described in Section 4.4.

4.1. One set of parallel rays. No refraction

It is possible to obtain a formula for the error in wave amplitude for a single set of parallel rays at infinite ray density. This formula is in terms of the length per wavelength of the sides of the squares (d/λ) and the angle between the rays and the sides of the squares (α). Figure 2

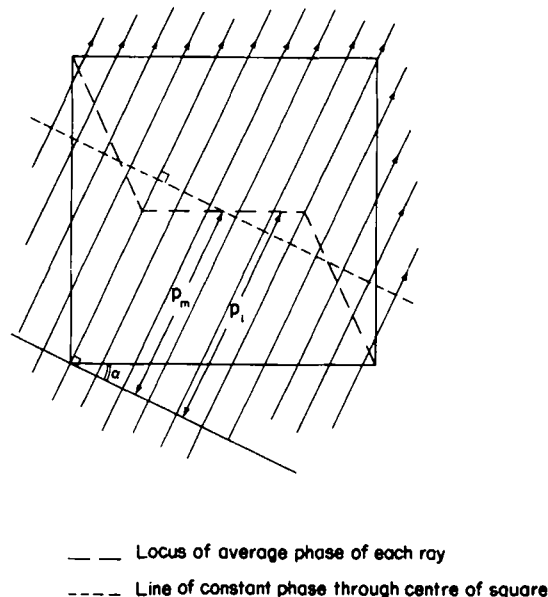


Figure 2. Average phases of a set of parallel rays crossing an averaging square

shows one set of rays crossing an averaging square at an arbitrary angle α . Because of symmetry, only values of α between 0° and 45° need be considered.

For N rays crossing an averaging square, the average wave amplitude and phase in the square are

$$A_{av}e^{iS_{av}} = \left(Ae^{ik[P_m+(P_1-P_m)]} \frac{q_1b}{d^2} + Ae^{ik[P_m-(P_1-P_m)]} \frac{q_1b}{d^2} \right) \\ + \left(Ae^{ik[P_m+(P_2-P_m)]} \frac{q_2b}{d^2} + Ae^{ik[P_m-(P_2-P_m)]} \frac{q_2b}{d^2} \right) + \dots \text{ to } N/2 \text{ terms} \quad (26)$$

In this equation:

1. Each wave amplitude A has been weighted in proportion to the ray's region of influence in the averaging square (factor qb/d^2)
2. Corresponding rays either side of the centre ray have been paired together
3. P_m and P_1, P_2 , etc. are defined in Figure 2.

Evaluating the pair of terms in each bracket and taking the limit as $N \rightarrow \infty$:

$$A_{av}e^{iS_{av}} = \lim_{N \rightarrow \infty} Ae^{ikP_m} \frac{2b}{d^2} \sum_{i=1}^{N/2} q_i \cos k(P_i - P_m) \quad (27)$$

Equation (27) shows that the averaging method predicts the phase correctly (this is obvious from the symmetry about the centre ray) but the amplitude A is altered from its correct value by the factor

$$\frac{A_{av}}{A} = \lim_{N \rightarrow \infty} \frac{2b}{d^2} \sum_{i=1}^{N/2} q_i \cos k(P_i - P_m) \\ = \frac{2}{d^2} \int_{\text{extreme ray}}^{\text{centre ray}} q \cos k(P - P_m) db \quad (28)$$

This integral can be evaluated in terms of the size per wavelength of the averaging square (d/λ) and the ray angle (α). The result is:

$$\frac{A_{av}}{A} = \frac{2}{\pi(d/\lambda)^2} \left(\frac{(d/\lambda) \sin(2\theta \sin \alpha)}{2 \sin \alpha (\cos^2 \alpha - \sin^2 \alpha)} \right. \\ \left. + \frac{2 \sin \alpha \cos \alpha \sin[\theta(\cos \alpha + \sin \alpha)] \sin[\theta(\cos \alpha - \sin \alpha)]}{\pi(\cos^2 \alpha - \sin^2 \alpha)^2} \right) \quad (29)$$

where

$$\theta = \frac{\pi(d/\lambda)(\cos \alpha - \sin \alpha)}{2 \cos \alpha} \quad (30)$$

Using equation (29), A_{av}/A has been calculated for values of d/λ from 0.25 to 2.5 at intervals of 0.25 and for values of α from 0° to 45° at 1° intervals. For each value of d/λ , A_{av}/A shows a single minimum with respect to α , increasing to 1 at $\alpha = 0^\circ$ and 45° . Table I lists the minimum A_{av}/A (and the corresponding percentage error) for each value of d/λ and the α at which it occurred. It can be seen that as d/λ is increased there is a systematic decrease in A_{av}/A from the correct value of 1. This error trend is to be expected because, as errors in determining the mean phase of each ray increase, the effect is that rays in the same wave train will combine in an increasingly random-phase manner.

These results indicate that to keep amplitude errors within 5 per cent, the square size per wavelength should not be greater than about 0.75.

Table I. Theoretical square-averaging amplitudes for a single parallel set of rays. Shows the minimum value of A_{av}/A (equation (29)) and the corresponding percentage error and ray angle (α) for different square sizes per wavelength (d/λ)

$\frac{d}{\lambda}$	Minimum A_{av}/A	Percentage error of minimum A_{av}/A	α at minimum A_{av}/A (degrees)
0.25	0.992	-0.8	19
0.5	0.970	-3.0	19
0.75	0.934	-6.6	19
1.0	0.887	-11.3	20
1.25	0.829	-17.1	20
1.5	0.765	-23.5	21
1.75	0.694	-30.6	21
2.0	0.620	-38.0	22
2.25	0.544	-45.6	22
2.5	0.468	-53.2	23

4.2. Several sets of rays. No refraction

In the first part of this section, the error in the total wave amplitude for several intersecting plane wave trains in an averaging square is considered theoretically. Results from a ray model run at different square sizes per wavelength are then presented.

Consider n sets of rays crossing an averaging square in which the correct wave amplitude of each wave train is A_i and the calculated amplitude has an error δA_i . It has already been shown that there is no error in the phase S_i for sets of straight parallel rays. From linear superposition, the total amplitude error, δA , can be determined as

$$\delta A = \left(\sum_{i=1}^n \sum_{j=1}^n \delta A_i \delta A_j \cos(S_i - S_j) \right)^{1/2} \quad (31)$$

This can be expressed as a fraction of the correct total wave amplitude, A .

$$\frac{\delta A}{A} = \left(\frac{\sum_{i=1}^n \sum_{j=1}^n \frac{\delta A_i}{A_i} \frac{\delta A_j}{A_j} (A_i A_j \cos(S_i - S_j))}{\sum_{i=1}^n \sum_{j=1}^n A_i A_j \cos(S_i - S_j)} \right)^{1/2} \quad (32)$$

If the waves destructively interfere to give a total wave amplitude close to zero, it becomes meaningless to give δA as a fraction of A . For small A , it is more meaningful to express δA as a fraction of the total random-phase amplitude $A_{rp} = \sqrt{(\sum_{i=1}^n A_i^2)}$, provided no two of the waves are phase-locked. This fractional error can be written as

$$\frac{\delta A}{A_{rp}} = \left(\frac{\sum_{i=1}^n \delta A_i^2}{\sum_{i=1}^n A_i^2} + \frac{\sum_{i=1}^n \sum_{j=1 (i \neq j)}^n \frac{\delta A_i}{A_i} \frac{\delta A_j}{A_j} (A_i A_j \cos(S_i - S_j))}{\sum_{i=1}^n A_i^2} \right)^{1/2} \quad (33)$$

Equation (32) is used for $A \geq A_{rp}$ and equation (33) for $A \leq A_{rp}$. The condition $A \leq A_{rp}$ can be expressed alternatively as

$$\sum_{i=1}^n \sum_{j=1 (i \neq j)}^n A_i A_j \cos(S_i - S_j) \leq 0 \quad (34)$$

Some qualitative conclusions can be drawn from equation (32) and (33) about the total fractional amplitude error in comparison with the worst fractional amplitude error of the individual wave trains $(\delta A_i/A_i)_{\max}$.

1. Equation (32) has the form of a weighted average of $(\delta A_i/A_i)(\delta A_j/A_j)$. If the 'weights' are all positive, $\delta A/A$ is clearly no worse than $(\delta A_i/A_i)_{\max}$. Although equation (32) is used when the wave trains tend to be in phase, it is possible that some of the 'weights' may be negative and combine in such a way to give a fractional amplitude error greater than $(\delta A_i/A_i)_{\max}$.
2. Equation (33) is used for the case where the waves tend to be out of phase and the inequality 34 holds. Usually, therefore, the second term on the right of equation (33) will be negative. If this is so, then $\delta A/A_{rp}$ is less than $(\delta A_i/A_i)_{\max}$. However, there is a small probability that the second term on the right of equation (33) could be positive and cause $\delta A/A_{rp}$ to be greater than $(\delta A_i/A_i)_{\max}$.

The problem of diffraction around a semi-infinite breakwater on a constant-depth sea bed was chosen for the ray model investigation.² The semi-infinite breakwater problem is well suited for this purpose because it involves the interference of several wave trains and because it is possible to obtain at any point the exact total wave amplitude predicted by the ray method. The wave trains in this problem are (Figure 3):

- (a) A set of parallel rays in the open zone representing the incident wave.
- (b) A set of diverging rays originating on the shadow boundary travelling into the sheltered zone.
- (c) A set of diverging rays originating on the shadow boundary travelling into the open zone. The sets of rays in (b) and (c) represent the diffracted incident wave and are symmetric about the shadow boundary.
- (d) A set of diverging rays from the tip of the breakwater representing the diffracted reflected wave.

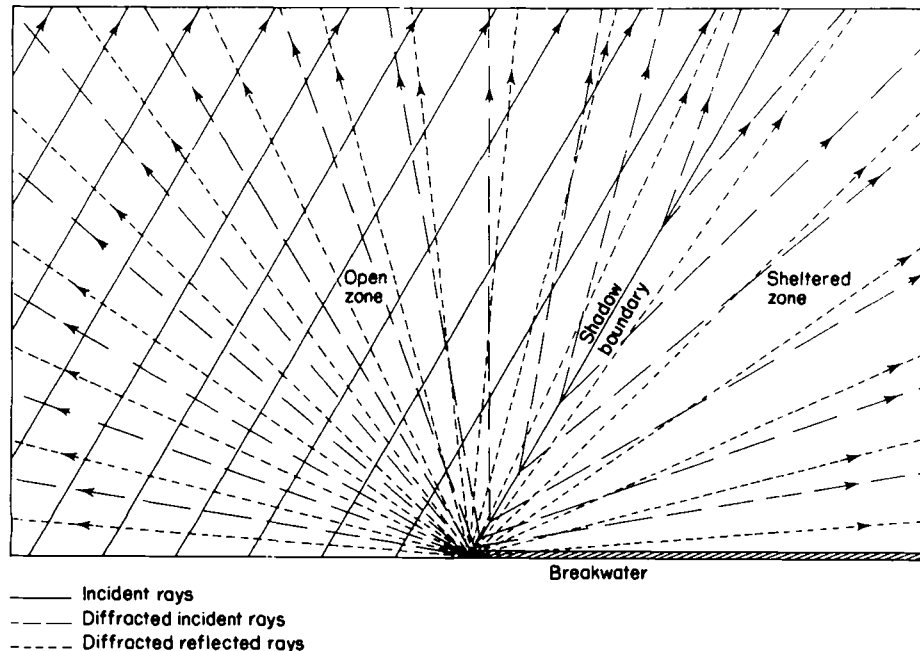


Figure 3. Ray diagram for the semi-infinite breakwater problem

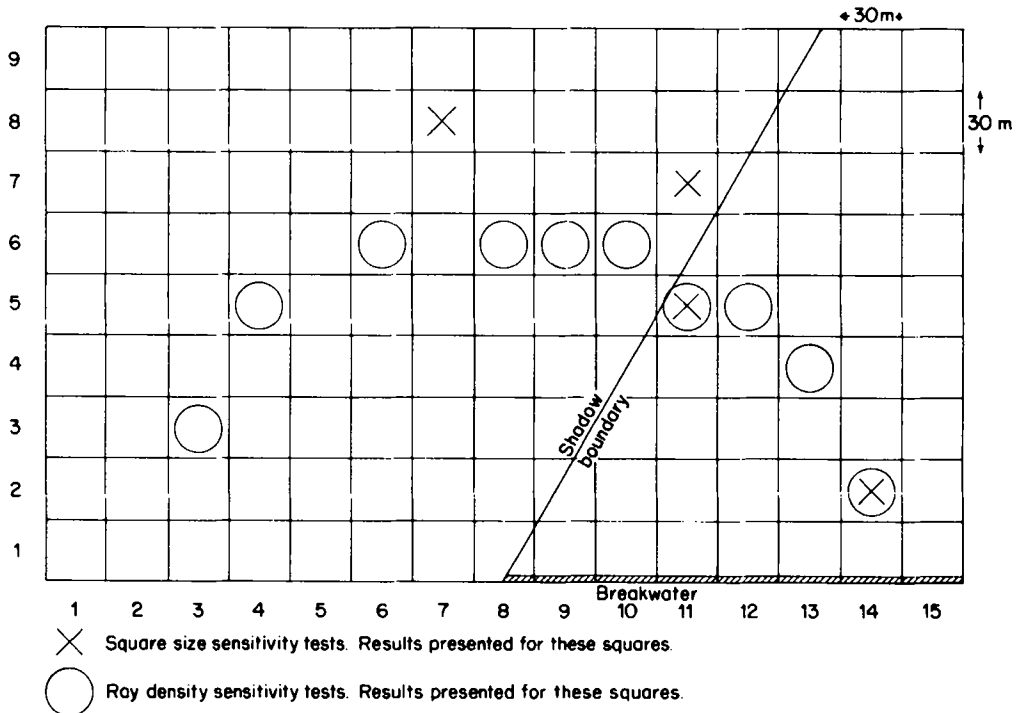


Figure 4. Ray model grid for tests with a semi-infinite breakwater on a flat sea bed. Incident angle 60°

A grid of 15 by 9 squares was used with the breakwater lying along one of the long boundaries with the tip at the centre of the boundary (Figure 4). Separate runs were performed with square sizes per wavelength (d/λ) of 0.25 to 2.5 at 0.25 intervals. Different d/λ were obtained by altering the wavelength. A ray density of about 20 rays per grid side ensured that inadequate density of rays did not contribute significantly to the total error. The exact total wave amplitudes given by the ray method were calculated at the centre of the averaging squares in order that a comparison with the model results could be made. These exact ray method amplitudes are all in close agreement with Sommerfeld's analytical solution.^{2,19}

Results are presented at four averaging squares, each in a different wave regime. Squares 14, 2 and 7, 8 are well into the sheltered and open zones, respectively, and squares 11, 5 and 11, 7 are close to the shadow boundary on either side of it (Figure 4). Figures 5–8 show the exact ray method amplitudes and the model amplitudes at each d/λ in each of the four squares. Tables II–V show the model fractional amplitude error, $\delta A/A$ (expressed as a percentage) and the theoretical fractional error (29) for the wave train that crosses at the worst angle. Also shown in these Figures and Tables are results using the circumcircle phase correction discussed in Section 4.4.

The following observations are made on the results:

1. *Square 14, 2 (Figure 5 and Table II).* In this square there are two sets of diverging rays (representing the diffracted incident and diffracted reflected wave trains) almost in phase and travelling very nearly in the same direction. It would be expected from equation (32) that $\delta A/A$ would be very close to the individual fractional amplitude errors. This is seen to be the

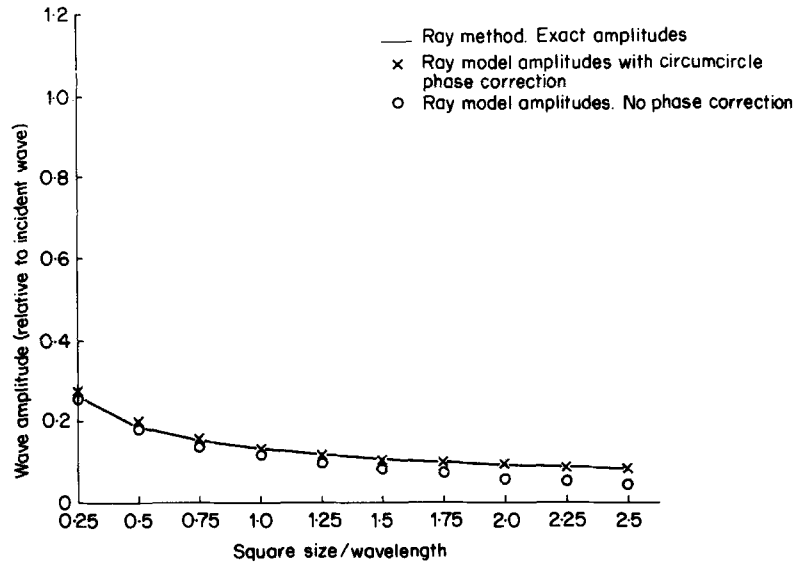


Figure 5. Variation of wave amplitude with square size per wavelength (d/λ). Semi-infinite breakwater, flat sea bed. Square 14, 2

case. The fact that the rays are diverging rather than parallel seems to have little effect on $\delta A/A$.

2. *Square 7, 8* (Figure 6 and Table III). The incident wave has a far larger amplitude than the diffracted waves and also has the largest fractional amplitude error. It would be expected that the total fractional amplitude error would be very similar to the fractional amplitude error of the incident wave alone. Table III shows this to be so.

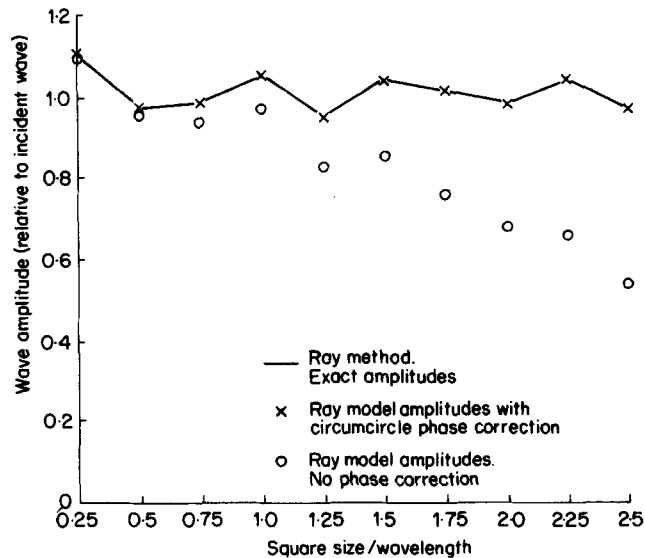


Figure 6. Variation of wave amplitude with square size per wavelength (d/λ). Semi-infinite breakwater, flat sea bed. Square 7, 8

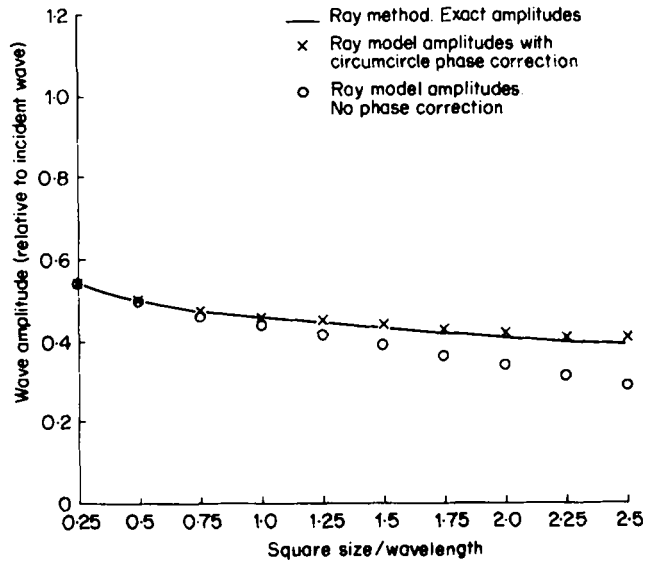


Figure 7. Variation of wave amplitude with square size per wavelength (d/λ). Semi-infinite breakwater, flat sea bed. Square 11, 5

3. *Square 11, 5* (Figure 7 and Table IV). This square lies in the sheltered zone close to the shadow boundary. In this region there are two sets of rays (diffracted incident and diffracted reflected waves) nearly in phase but travelling in significantly different directions (between about 4° and 13° depending on the wavelength). The worst fractional amplitude error occurs for the diffracted reflected wave for all the wavelengths considered. Because of

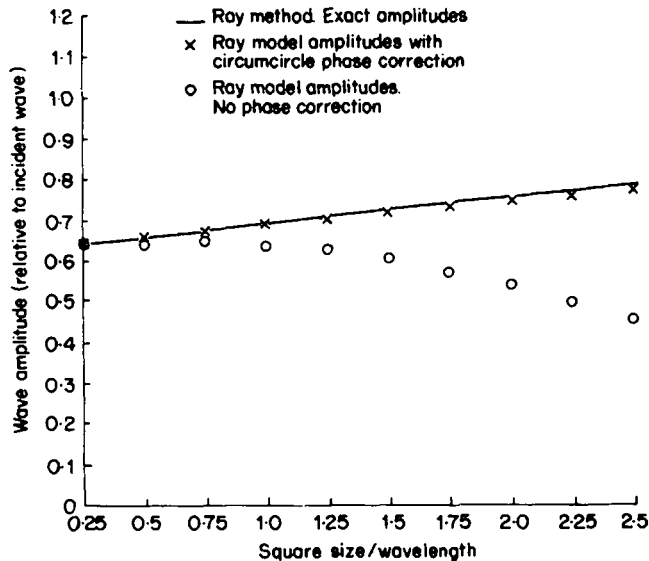


Figure 8. Variation of wave amplitude with square size per wavelength (d/λ). Semi-infinite breakwater, flat sea bed. Square 11, 7

Table II. Square 14, 2. Semi-infinite breakwater, flat sea bed. Percentage error of square-averaging amplitude relative to exact ray method amplitude at different square sizes per wavelength (d/λ). Worst ray angle ($\alpha = 14^\circ$) occurs for both the diffracted incident wave and the diffracted reflected wave

$\frac{d}{\lambda}$	Percentage error theoretical worst wave train	Percentage error square averaging	Percentage error square averaging with phase correction
0.25	-0.7	-0.4	0.4
0.5	-2.8	-2.7	0
0.75	-6.1	-5.8	0
1.0	-10.4	-9.7	0
1.25	-15.3	-15.0	0
1.5	-20.6	-20.0	0
1.75	-26.0	-26.5	0
2.0	-31.4	-31.6	0
2.25	-36.6	-36.7	0
2.5	-41.7	-42.4	0

the similar phases but different $\delta A_i/A_i$ of the two waves, equation (32) predicts that the total fractional amplitude error, $\delta A/A$, will be somewhat less than the worst $\delta A_i/A_i$. The model results in Table IV agree with this prediction.

4. *Square 11, 7 (Figure 8 and Table V)*. There are three wave trains crossing this square: the incident wave, the diffracted incident wave (out of phase with the incident wave by close to π) and the diffracted reflected wave (nearly in phase with the incident wave). The incident and diffracted incident waves are phase-locked and therefore equation (32) should be used in evaluating $\delta A/A$. When one wave train is out of phase with the others, it is not immediately clear from equation (32) whether $\delta A/A$ should be greater or less than the worst $\delta A_i/A_i$ (which, in this case, is for the diffracted reflected wave). Table V shows that $\delta A/A$ is somewhat less.

Table III. Square 7,8. Semi-infinite breakwater, flat sea bed. Percentage error of square-averaging amplitude relative to exact ray method amplitude at different square sizes per wavelength (d/λ). Worst ray angle ($\alpha = 30^\circ$) occurs for the incident wave

$\frac{d}{\lambda}$	Percentage error theoretical worst wave train	Percentage error square averaging	Percentage error square averaging with phase correction
0.25	-0.5	-0.5	0.1
0.5	-2.1	-2.0	0.1
0.75	-4.7	-4.8	-0.1
1.0	-8.2	-7.9	0.1
1.25	-12.7	-12.9	0
1.5	-17.9	-17.8	-0.1
1.75	-23.8	-23.5	0.2
2.0	-30.3	-30.5	-0.3
2.25	-37.1	-36.5	0.1
2.5	-44.4	-44.9	0.1

Table IV. Square 11, 5. Semi-infinite breakwater, flat sea bed. Percentage error of square-averaging amplitude relative to exact ray method amplitude at different square sizes per wavelength (d/λ). Worst ray angle ($\alpha = 34^\circ$) occurs for the diffracted reflected wave

$\frac{d}{\lambda}$	Percentage error theoretical worst wave train	Percentage error square averaging	Percentage error square averaging with phase correction
0.25	-0.4	-0.2	0
0.5	-1.5	-1.0	0.2
0.75	-3.3	-2.1	0.4
1.0	-5.8	-4.0	0.9
1.25	-8.9	-6.4	1.6
1.5	-12.7	-9.1	1.9
1.75	-17.0	-12.7	2.4
2.0	-21.8	-17.2	2.9
2.25	-27.1	-21.6	3.5
2.5	-32.7	-26.6	4.1

These results are in agreement with the theoretical conclusion that the total fractional amplitude error for several intersecting wave trains will only rarely be greater than the worst fractional amplitude error among the individual wave trains.

4.3. One set of parallel rays. Refraction present

The semi-infinite breakwater problem cannot be used for testing the grid size sensitivity on a varying depth sea bed (i.e. with refraction) since it is not possible to obtain exact ray method values at the centres of the averaging squares. Instead, the simpler problem of a single plane wave train propagating over a parallel-contoured sea bed is considered. A 15 by 9 grid of square elements is used with a linear variation of depth as shown in Figure 9. In this problem, exact results at the centres of the averaging squares can be obtained from Snell's law of refraction and equations (3) and (9).

Table V. Square 11, 7. Semi-infinite breakwater, flat sea bed. Percentage error of square-averaging amplitude relative to exact ray method amplitude at different square sizes per wavelength (d/λ). Worst ray angle ($\alpha = 25^\circ$) occurs for the diffracted reflected wave

$\frac{d}{\lambda}$	Percentage error theoretical worst wave train	Percentage error square averaging	Percentage error square averaging with phase correction
0.25	-0.7	0.2	0.5
0.5	-2.7	-1.5	0.2
0.75	-6.0	-4.0	-0.4
1.0	-10.4	-7.5	-0.4
1.25	-15.9	-11.5	-0.8
1.5	-22.3	-16.4	-1.0
1.75	-29.2	-22.2	-1.2
2.0	-36.7	-28.5	-1.4
2.25	-44.5	-35.1	-1.6
2.5	-52.3	-42.5	-1.8

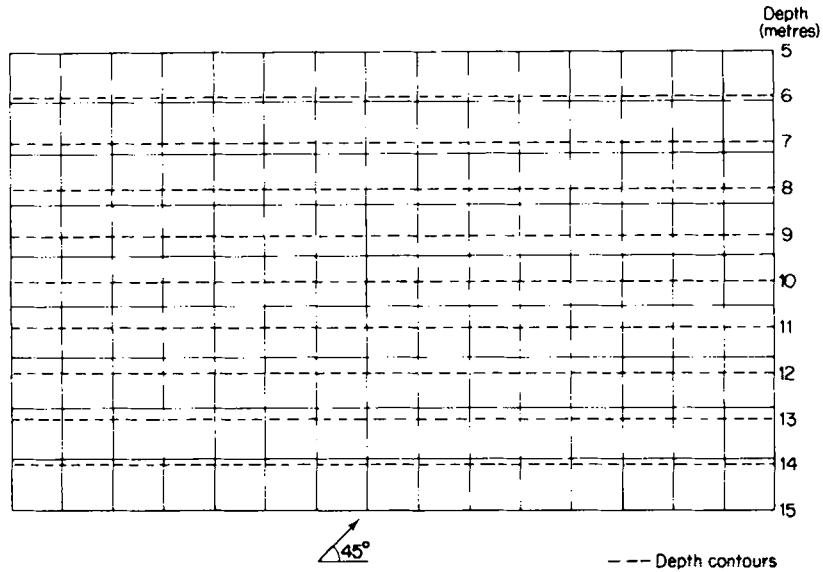


Figure 9. Ray model grid and bathymetry for tests with a parallel-contoured sea bed. Incident angle 45°

The same values of grid size per wavelength (d/λ) as those in the previous section were tested ($d/\lambda = 0.25$ to 2.5 at 0.25 intervals) but with an incident wave angle of 45° . Since it was necessary that rays should undergo the same amount of refraction in each run with different d/λ , the variation of wavelength over the whole grid had to be the same for each of these runs. This meant that d/λ could only be changed by altering the square size. The incident wave period was chosen so that the wavelength which gave the desired value of d/λ

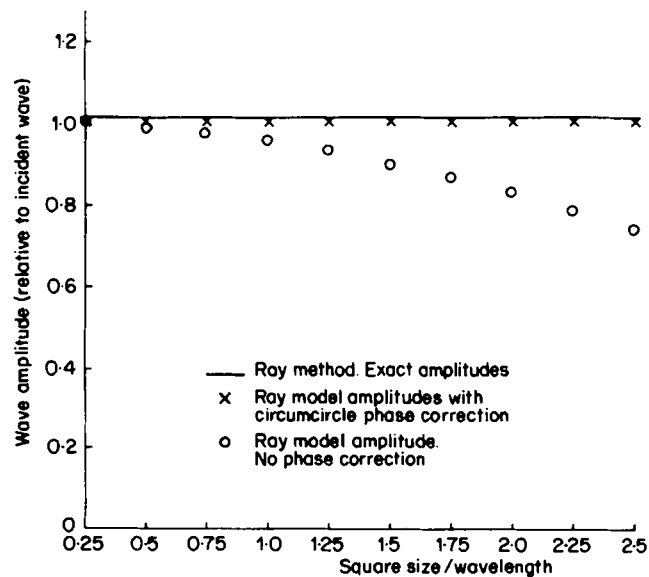


Figure 10. Variation of wave amplitude with square size per wavelength (d/λ). Single plane wave train, parallel contoured sea bed. Average of amplitudes in squares in fifth row

Table VI. Average of squares on fifth row. Single wave train, parallel contoured sea bed. Percentage error of square-averaging amplitude relative to exact ray method amplitude at different square sizes per wavelength (d/λ). Ray angle for flat bed theoretical errors is the ray angle at the 10 m depth contour in the model ($\alpha = 36^\circ$)

$\frac{d}{\lambda}$	Percentage error theoretical worst wave train	Percentage error square averaging	Percentage error square averaging with phase correction
0.25	-0.3	-1.0	-0.7
0.5	-1.1	-1.9	-0.7
0.75	-2.5	-3.5	-0.7
1.0	-4.4	-5.2	-0.7
1.25	-6.8	-7.8	-0.8
1.5	-9.7	-10.8	-0.8
1.75	-13.1	-14.1	-0.8
2.0	-16.9	-18.2	-0.9
2.25	-21.1	-22.4	-0.9
2.5	-25.6	-27.0	-0.9

occurred at a depth of 10 m (which is at the centre of the fifth row of squares). A ray density of 20 rays per square side was used.

Figure 10 shows the model wave amplitudes (averaged over all squares in the fifth row) for each d/λ . The percentage error relative to the amplitude determined from Snell's law is shown in Table VI. Also shown in this Table is the theoretical percentage error determined from equation (29) assuming a flat sea bed and a ray angle equal to that at the 10 m depth contour in the model. Table VI shows that the model errors are only slightly greater than the theoretical errors. These small additional errors, resulting from the presence of curved rays, can be accounted for in two ways.

1. The locus of the mid-points of a set of curved rays crossing a square will be different from the locus of the mid-points of a set of straight rays.
2. The average of the phases of a curved ray at the entry and exit points in a square will be different from the phase at the mid-point.

4.4. Circumcircle phase correction

It has been shown that, by taking the mean phase between the entry and exit points of rays crossing an averaging square, the maximum allowable square size is about 0.75 wavelength. This limit gives errors in wave amplitude of around 5 per cent for the worst ray angles. Although this limit is considerably larger than those in finite element or finite difference models (maximum element size about 0.17 wavelength) it will still lead to high data preparation time, computing storage and run time for short waves in large sea areas. The sensitivity analysis has shown that by far the largest contribution to this error has arisen from the simple geometrical consideration that the entry and exit points in a *square* were used to determine the mean phase of each ray. The influences of intersecting sets of rays and refraction have been shown to be much smaller.

The idea of the circumcircle phase correction is to extrapolate a ray's path onto the circumcircle of the averaging square. The intersections of the ray with the circumcircle are then used to determine the mean phase. It is assumed that the extrapolated ray paths

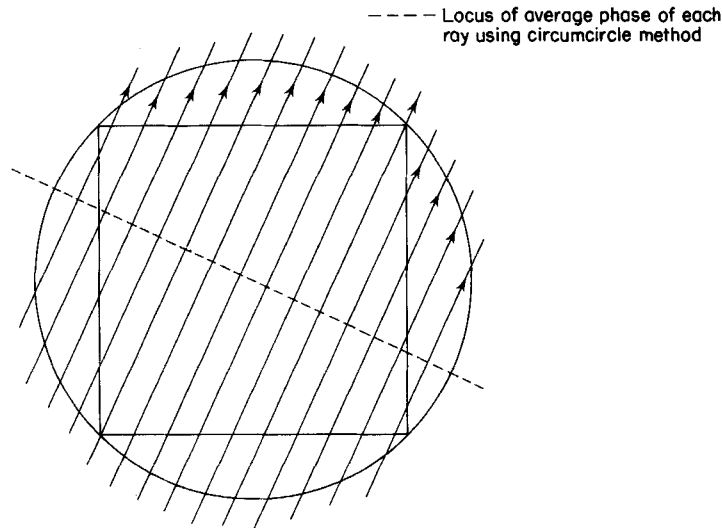


Figure 11. Average phases of a set of parallel rays crossing an averaging square with the circumcircle phase correction

between the entry/exit points on the square and the entry/exit points on the circumcircle are straight. The determination of the intersections of the ray with the circumcircle then reduces to the simple problem of finding the intersections of two known straight lines with a known circle. This process does, of course, add to the run time in plotting each ray.

The circumcircle method removes completely the error arising from taking the mean phase between the entry and exit points on a square. Consider a single set of straight, parallel rays crossing an averaging square with their paths extrapolated to the circumcircle (Figure 11). It is obvious that the mean phase of each ray determined by the circumcircle method is exactly the value at the centre of the averaging square, whatever the ray angle and square size. An analysis for infinite ray density, corresponding to that in Section 4.1, therefore shows zero error in amplitude for all ray angles and square sizes.

It remains to see how this idea works in practice. The tests in Section 4.2 (semi-infinite breakwater on a horizontal sea bed) and Section 4.3 (single wave train on parallel contoured sea bed) were repeated using the circumcircle method. Figures 5–8 and 10 and Tables II–VI show the results. A big improvement is obtained over the corresponding results without the circumcircle phase correction. At the largest square size per wavelength ($d/\lambda = 2.5$), the worst amplitude error amongst the squares considered is about 4 per cent with the circumcircle method. The other squares show much smaller errors. Without the circumcircle phase correction, the averaging method breaks down completely giving errors of over 40 per cent in the worst cases. Depending on the required accuracy in any problem, even larger square sizes than 2.5 wavelengths could be used. It was found that the extra computation required by the circumcircle method lead to an increase in run time of 17 per cent but this, of course, will be greatly offset in practical problems by the savings in using larger square sizes.

5. SENSITIVITY OF SQUARE AVERAGING TO RAY DENSITY

The accuracy of the square averaging method clearly depends on the number of rays in each wave train crossing a square. This applies to both square averaging with phasing and square

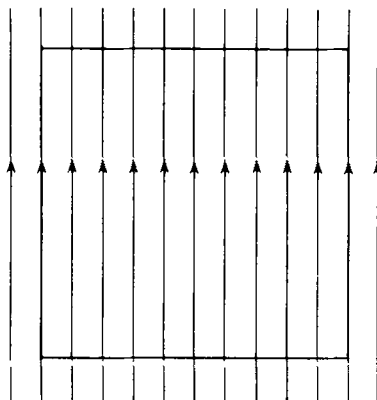


Figure 12. An example of a set of rays crossing an averaging square giving a large ray density error

averaging without phasing. A particularly large amplitude error resulting from insufficient ray density occurs in the simple example shown in Figure 12. A single set of straight parallel rays crosses an averaging square parallel to two sides of the square. The maximum error occurs when two rays just graze the two sides of the square, as shown in Figure 12. The amplitude error for this case can be calculated from equation (15) (with phasing) and equation (24) (without phasing) for a general ray density of n rays per square side. These amplitude errors, expressed as a fraction, are:

$$\frac{1}{n} \quad \text{with phasing}$$

$$1 - \left(1 - \frac{1}{n}\right)^{1/2} \quad \text{without phasing}$$

This shows that larger errors are given by the method of averaging with phasing.

This example, of course, is an extreme case and smaller errors can be expected in practice. The semi-infinite breakwater problem again provides a good test of the sensitivity to ray density when there are several intersecting wave trains. The same model set-up as before (Section 4.2) was used, with an incident wave angle of 60° (Figure 4) and square size per wavelength of 0.25. Separate runs were performed for ray densities (expressed as the number of rays, n , per grid side) of 1 to 6 at intervals of 1, and 6 to 12 at intervals of 2. The angular separation of the diverging diffracted rays was chosen so that their density was roughly equal to the density of the parallel incident rays at a distance of one and a half wavelengths from the breakwater tip. Results in averaging squares at about this distance from the breakwater tip were used for comparison with the exact ray method values.

Table VII shows the percentage amplitude errors in ten of these averaging squares (Figure 4) for each of the ray densities. Two general trends can be seen from this Table:

1. For a particular ray density, there is considerable variation in amplitude error from square to square. This becomes more marked at the lower ray densities.
2. For a particular averaging square, the amplitude error tends to increase unsystematically as the ray density is decreased.

These trends are to be expected. As the ray density is decreased, it becomes a question of chance as to whether rays cross a square in such a way as to produce a small or large amplitude error. It would appear that a ray density as low as four or five rays per square side does not generally give errors greater than 5 per cent.

Table VII. Semi-infinite breakwater, flat sea bed. Percentage error of square-averaging amplitude relative to exact ray method amplitude at different ray densities

Square co-ordinates	Percentage amplitude error								
	Ray density = 12	Ray density = 10	Ray density = 8	Ray density = 6	Ray density = 5	Ray density = 4	Ray density = 3	Ray density = 2	Ray density = 1
14, 2	0	0	-0.4	-1.1	-1.1	-1.9	-6.9	-1.9	12.6
13, 4	0.3	0	0	-1.2	-0.6	-0.6	3.0	-2.1	30.0
12, 5	0.2	0.2	-0.5	-1.4	-1.1	-1.6	4.1	-1.1	65.9
11, 5	0.2	0	-0.9	-1.3	-3.7	-6.1	-10.7	-17.0	-69.1
10, 6	-0.4	-0.7	-1.3	-1.6	-2.4	1.1	3.6	-18.8	-42.2
9, 6	-0.7	-1.3	0	-0.2	2.6	-3.8	-4.9	9.6	-27.6
8, 6	-0.5	-0.5	-0.5	-0.6	-0.1	-0.7	-0.5	-0.4	-1.2
6, 6	-0.6	-0.5	-0.6	-0.3	0.8	-0.4	-5.4	0.8	9.6
4, 5	-0.7	-0.7	-0.7	-0.7	0.7	-0.7	1.9	-0.9	8.7
3, 3	-0.5	-0.5	-0.5	-0.6	-1.8	-0.5	-0.7	-0.4	15.0

6. SUMMARY AND CONCLUSIONS

Computational ray methods are used in coastal and harbour wave disturbance modelling where the area to be modelled is large compared to the wavelength. A technique of spatial averaging of rays has been described. This technique involves averaging the effects of rays crossing each square element of a grid covering the sea area under study. By choosing this square grid to be identical with the grid containing depth data, the square averaging technique can be easily incorporated into existing ray plotting routines. The square averaging technique has a number of positive features which make it preferable to the usual method of evaluating refraction and shoaling coefficients along each ray.

1. Caustics and ray crossings are automatically smoothed.
2. The interference between several wave trains is calculated with the options of either taking into account the relative phases of the wave trains or of treating them as random.
3. Wave amplitudes in squares partially covered by sets of rays are correctly predicted when the relative phases of wave trains are taken into account.
4. Wave amplitudes are obtained in a regular array over the whole sea area under study.

A technique of averaging rays crossing a segment of a line is very similar, but has the disadvantage of breaking down when rays make a very acute angle with the line.

Sensitivity tests have been carried out to determine the accuracy of the predicted wave amplitude with respect to:

1. the square size per wavelength (for the case when the relative phases of wave trains are taken into account), and
2. the ray density.

A square size of 0.75 wavelength was found to give errors of around 5 per cent. Much more accurate wave amplitudes were obtained by incorporating a phase correction method. With this method a square size of 2.5 wavelengths gave an error of 4 per cent in the worst case. At most other squares the error was considerably less than this. A ray density of about five rays per square side was shown to give errors generally no worse than 5 per cent.

ACKNOWLEDGEMENTS

This work was supported by the Department of Transport as part of an overall programme of research into the response of harbours. The paper is published with the permission of the Managing Director of Hydraulics Research Station Limited.

The author wishes to acknowledge the help and encouragement of Dr E. C. Bowers in this work.

REFERENCES

1. E. C. Bowers and H. N. Southgate, 'Wave diffraction, refraction and reflection. A comparison between a physical model and a mathematical ray model', *Internal Report 240*, Hydraulics Research Station, Wallingford, Oxon, U.K., November 1982.
2. H. N. Southgate, 'Ray methods for combined refraction and diffraction problems', *Internal Report 214*, Hydraulics Research Station, Wallingford, Oxon, U.K., July 1981.
3. M. B. Abbott, H. M. Petersen and O. Skovgaard, 'On the numerical modelling of short waves in shallow water', *Journal of Hydraulic Research*, **16** (3), 173-204 (1978).
4. Y. Ito and K. Tanimoto, 'A method of numerical analysis of wave propagation. Application to wave diffraction and refraction', *Proceedings of the 13th International Conference on Coastal Engineering, Vancouver, ASCE*, **1**, 503-522 (1973).
5. J. C. W. Berkhoff, 'Computation of combined refraction and diffraction', *Proceedings of the 13th International Conference on Coastal Engineering, Vancouver, ASCE*, **1**, 471-490 (1973).
6. P. Bettess and O. C. Zienkiewicz, 'Diffraction and refraction of surface waves using finite and infinite elements', *International Journal for Numerical Methods in Engineering*, **11**, 1271-1290 (1977).
7. J. R. Houston, 'Combined refraction and diffraction of short waves using the finite element method', *Applied Ocean Research*, **3** (4), 163-170 (1981).
8. C. J. Lozano and P. L-F. Liu, 'Refraction-diffraction model for linear surface water waves', *Journal of Fluid Mechanics*, **101** (4), 705-720 (1980).
9. A. C. Radder, 'On the parabolic equation method for water-wave propagation', *Journal of Fluid Mechanics*, **95** (1), 159-176 (1979).
10. G. Gilbert and C. L. Abernethy, 'Refraction of wave spectra', *Internal Report 117*, Hydraulics Research Station, Wallingford, Oxon, U.K., May 1975.
11. A. H. Brampton, 'A computer method for wave refraction', *Internal Report 172*, Hydraulics Research Station, Wallingford, Oxon, U.K., December 1977.
12. W. H. Munk and R. S. Arthur, 'Wave intensity along a refracted ray', *Circular 521*, U.S. National Bureau of Standards, Washington, 1952.
13. J. C. W. Berkhoff, N. Booy and A. C. Radder, 'Verification of numerical wave propagation models for simple harmonic linear water waves', *Coastal Engineering*, **6**, 255-279 (1982).
14. Hydraulics Research Station, 'Suez Canal feasibility study', *External Report 771*, 1977.
15. J. C. W. Berkhoff, 'Mathematical models of simple harmonic linear water waves. Wave diffraction and refraction', *Publication No 163*, Delft Hydraulics Laboratory, Holland, 1976.
16. R. Smith and T. Sprinks, 'Scattering of surface waves by a conical island', *Journal of Fluid Mechanics*, **72** (2), 373-384 (1975).
17. I. G. Jonsson, 'The general wave equation and the refraction approximation', *Progress Report 49*, Institute of Hydrodynamics and Hydraulic Engineering, Technical University of Denmark, 11-20, August 1979.
18. O. Skovgaard and I. G. Jonsson, 'Computation of wave fields in the ocean around an island', *International Journal for Numerical Methods in Fluids*, **1**, 237-272 (1981).
19. A. Sommerfeld, 'Mathematische theorie der diffraktion', *Mathematische Annalen*, **47**, 317-374 (1896).